ICANS-XIV
14th Meeting of the International Collaboration on
Advanced Neutron Sources
June 14-19, 1998
Starved Rock Lodge, Utica, IL, USA

Incident Spectrum Determination for Time-of-Flight Neutron Powder Diffraction Data Analysis

J. P. Hodges, J. D. Jorgensen, S. Short and D. N. Argyriou
Materials Science Division, Argonne National Laboratory, Argonne, IL 60439.

J.W. Richardson, Jr.
Intense Pulsed Neutron Source, Argonne National Laboratory, Argonne, IL 60439.

Abstract

Accurate characterization of the incident neutron spectrum is an important requirement for precise Rietveld analysis of time-of-flight powder neutron diffraction data. Without an accurate incident spectrum the calculated model for the measured relative intensities of individual Bragg reflections will possess systematic errors. We describe a method for obtaining an accurate numerical incident spectrum using data from a transmitted beam monitor.

1. Introduction

With a multidetector diffractometer, which can be either electronically or geometrically focused, a focused diffraction data set is constructed by summing a number of histograms.[1,2] Each of these histograms is generated by one element of an extended array of detectors. The summing operation is made possible by time-focusing the individual histograms to a desired pseudo-time corresponding to a reference detector position, such that data for the same d-spacing are summed into the same data channel regardless of the neutron wavelength. Normally, the reference detector position is taken as the average scattering angle of the extended detector array.

2. Incident Spectrum Measurement

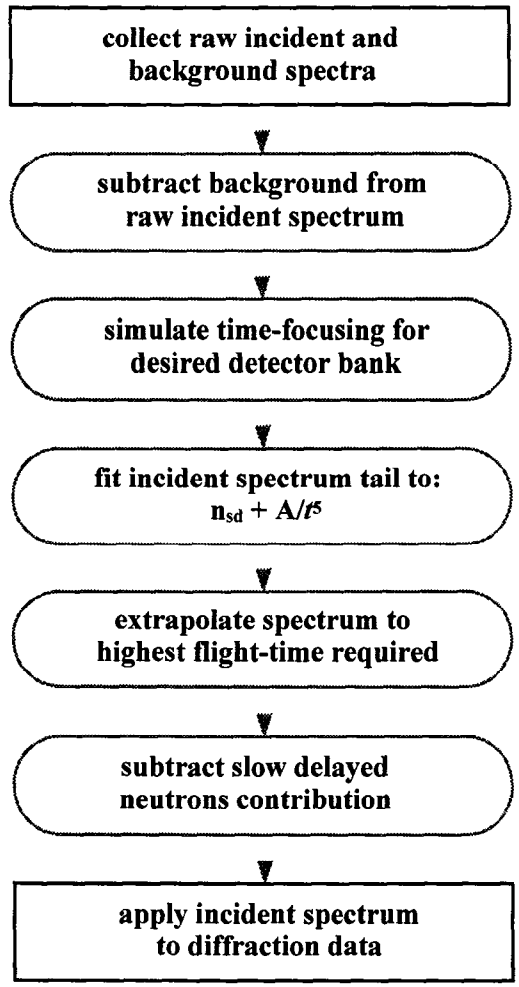

Fig. 1. A method for the construction of an effective incident spectrum.

An incident spectrum is a distribution of neutron flux versus a wavelength scale. However, for a focused time-of-flight diffractometer, the effective incident spectrum needed to model the data is a spectrum which, for any focused time (or *d*-spacing) channel, has been averaged over a range neutron wavelengths defined by the focusing operation. Features which are sharp in the actual incident spectrum, *e.g.* Bragg cutoffs due to window materials, are smoothed in the effective incident spectrum by the focusing operation. The determination of an effective incident spectrum for a particular diffraction data set is non-trivial because many aspects of the diffraction experiment can have an effect on the incident spectrum, *e.g.* sample environment, moderator temperature which can change with time, *etc.*.

The flow-chart presented in Fig. 1 displays a method for the construction of an effective incident spectrum that has proven to work well for the Special Environment Powder Diffractometer (SEPD) at IPNS. It should be possible to readily adapt this method to other time-of-flight neutron diffractometers.

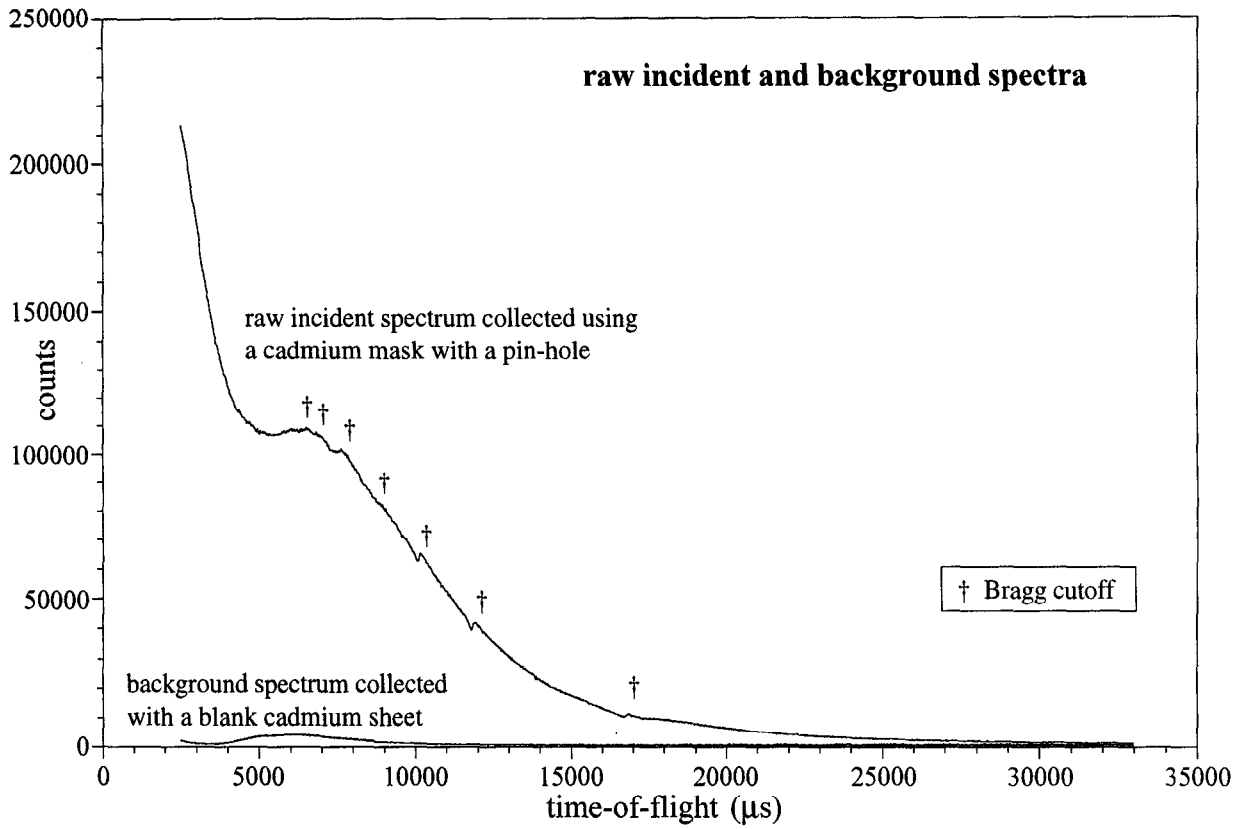

Fig. 2. Raw incident and background spectra collected on the SEPD.

Raw incident and background spectra, see Fig. 2, are collected in the transmitted neutron beam, downstream of the sample position, using a 10 atm He^3 proportional detector. A detector identical to those in the scattered detector banks is used so that minimal detector efficiency corrections (to be discussed later) are needed. The detector is shielded with B_4C except for a small hole for the transmitted beam. In order to prevent dead-time errors from saturation of the detector and/or associated electronics, a cadmium mask with a pin-hole (diameter $\approx$ 2 mm) is placed in front of the detector. To measure an incident spectrum applicable to normal data, no sample is placed in the sample position. The transmitted incident spectrum is first measured with the pin-hole in place. A background spectrum is also collected with a solid cadmium sheet of the same thickness in place of the pin-hole mask. The background spectrum is subtracted from the raw incident spectrum using the integrated counts in a low-efficiency upstream beam monitor to provide normalization. This yields an incident spectrum corrected for electronic, room background, and delayed neutrons with energies above the cadmium cutoff energy.

One clear advantage of measuring the incident spectrum using a transmitted beam detector, rather than the common approach of measuring the elastic incoherent scattering from vanadium in the sample position, is that the transmitted beam method will yield meaningful results for the normalization of data taken in special sample environments. In this case, the transmitted beam measurement is performed with the sample environment apparatus, *e.g.* pressure cell, furnace, *etc.*, in position. This yields an incident spectrum that includes the

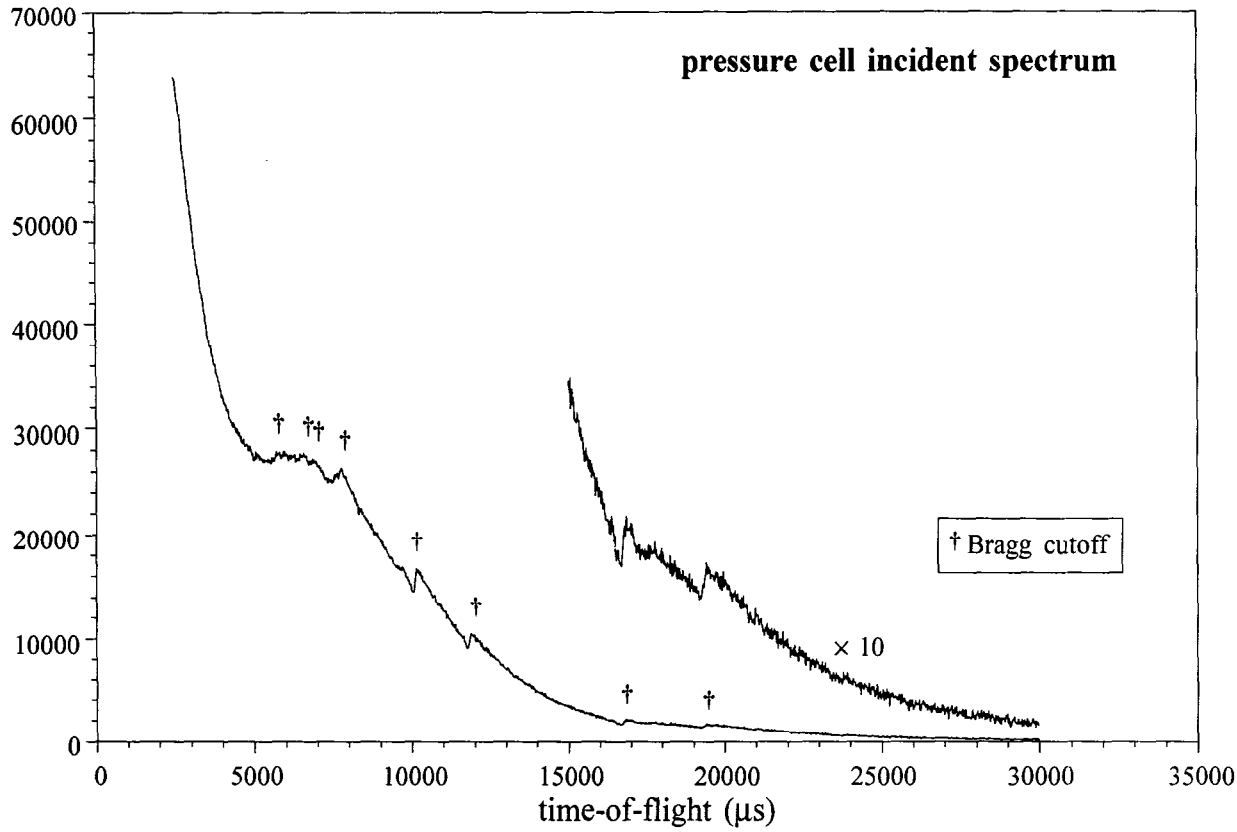

Fig. 3. Incident spectrum collected on the SEPD with a pressure cell in position.

attenuation of the neutron flux due to the presence of the apparatus in the incident and scattered beam. The attenuations are accurately measured if the transmitted and scattered paths through the apparatus are identical in composition and thickness. This is often the case, or very nearly so. Moreover, this can be used as a criteria in the design of special environment apparatus for use on a pulsed-source diffractometer. In Fig. 3 an incident spectrum that was measured with a high pressure cell in the sample position is shown. Large Bragg cutoffs due to the aluminum alloy pressure cell (adding to those from aluminum alloy windows along the flight path) appear as sharp features in the raw incident spectrum.

For special sample environments, the method of measuring the incident spectrum using a vanadium sample is not tractable because of multiple scattering. When the vanadium sample is placed inside the special environment apparatus, part of the detected neutrons result from multiple scattering involving the vanadium sample and the cell. This multiple scattering, which contaminates the measurement of the incident spectrum, cannot be directly measured because it disappears when the sample is removed; and methods for estimating its intensity and wavelength dependence are not sufficiently accurate to achieve the desired precision.

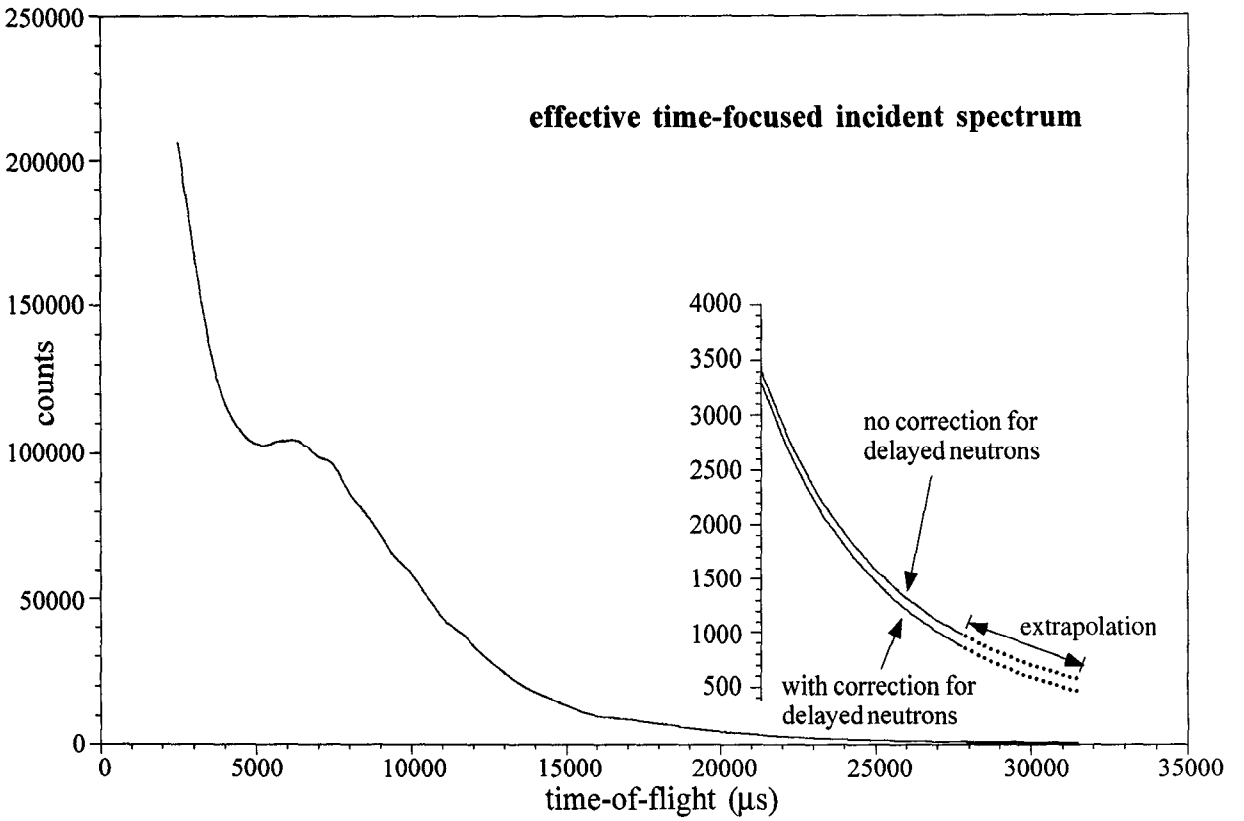

Fig. 4. An effective incident spectrum, that has been corrected for delayed neutrons and extrapolated to 31500 μs.

A second method we have used for estimating the slow delayed neutrons is based on trial-and-error methods to obtain the lowest R value in a Rietveld refinement. An estimate of the slow delayed neutrons is subtracted from the incident spectrum and a Rietveld refinement is performed using data from a standard material (such as Al_2O_3). This is repeated for different estimates of the slow delayed neutron contribution and the resulting R values from the refinements are plotted as a function of the assumed values for the slow delayed neutron flux expressed as a fraction of the total incident flux integrated over the usable time frame (typically 2500 to 30000 μs on the SEPD). A clear minimum in the R value indicates the correct slow delayed neutron fraction.

These two methods for determining the slow delayed neutron flux have yielded the same result. When expressed as a fraction of the total incident neutron flux over the time range 2500-30000 μs on the SEPD, the slow delayed neutron fraction is 0.0030. This value is consistent with what one would expect for the IPNS target, for which the total (slow + fast) delayed neutron fraction is estimated to be 0.0042.

Because of the physical arrangement of detectors on the SEPD, with the transmitted beam detector at a longer path length than the scattered detectors, the incident spectrum data do not extend to long enough times to correspond to the longest times measured in the scattered detector banks. The time window for the "focused" incident spectrum is further shorted because the

3. Simulating Time-Focusing

In order to generate an effective incident spectrum that can be applied to a time-focused diffraction data set collected from an extended detector array, a smoothing operation that corresponds to the time-focusing is applied to the measured incident spectrum. The parameters for the smoothing are determined by the geometrical layout of the diffractometer (defined by the incident and scattered neutron flight paths, and the positions of the various detectors plus sample). The i^{th} channel of the effective incident spectrum, I_i^{eff} , constructed to be used with data from a particular detector array, for the case $i = 0$ at zero time-of-flight, is given by

$$I_i^{\text{eff}} = \frac{1}{j_{\max} - j_{\min}} \sum_{j_{\min}}^{j_{\max}} I_j^{\text{inc}} \tag{1}$$

where I_j^{inc} is the j^{th} channel of the incident spectrum. The limits of the sum are given by

$$j_{\min} = i \, \frac{\Delta t_{\text{eff}}}{\Delta t_{\text{inc}}} \cdot \frac{\ell_s}{\ell_t} \cdot \frac{\sin\theta_{\min}}{\sin\theta_{\text{ref}}} \tag{2}$$

and

$$j_{\max} = i \, \frac{\Delta t_{\text{eff}}}{\Delta t_{\text{inc}}} \cdot \frac{\ell_s}{\ell_t} \cdot \frac{\sin\theta_{\max}}{\sin\theta_{\text{ref}}} \tag{3}$$

where Δt_{inc} is the channel width (in time) for the data collected at the transmitted beam detector, ℓ_t is the path length from the moderator to the transmitted beam detector, Δt_{eff} is the channel width for the effective incident spectrum (which is chosen to be equal to the channel width for the scattered data to be analyzed), ℓ_s is the path length from the moderator to the reference detector position, $\sin\theta_{\text{ref}}$ is the scattering angle for the reference detector, $\sin\theta_{\min}$ is the minimum angle for the extended detector array, and $\sin\theta_{\max}$ is the maximum angle for the extended detector array. The code that performs this smoothing also includes a small correction for detector efficiency. Although identical detectors are used in the transmitted and scattered positions, the pin-hole restricts the transmitted beam to passing through a full diameter of the detector, while the scattered neutrons can pass through any chord of the detectors. The correction for this small difference in efficiency is readily calculated.

Upon completion of these steps a "pseudo-time-focused" incident spectrum that corresponds to the time-focusing used in a particular detector array has been constructed. This spectrum has the general shape of the original incident spectrum but the sharp Bragg cutoffs have been smoothed into broad shallow steps and the statistical scatter has been greatly reduced. However, before this incident spectrum can be used to normalize scattered intensities it must be corrected for delayed neutrons.

4. Delayed Neutron Correction

When a uranium target is used at a pulsed neutron source (as is the case at IPNS), fission reactions produce a background of delayed neutrons that are moderated and emitted over a time scale that is very long compared to the pulsed time frame (1/30 s at IPNS). These delayed neutrons possess an energy spectrum almost identical to that of the prompt neutrons. However, their flux distribution is essentially time-independent over the time of a data frame. This results in a constant background of neutrons in both the measured sample diffraction data and incident spectrum. In the case of diffraction data that are analyzed by the Rietveld technique, this additional background in the scattered data is readily fit (along with the other contributions to the background which vary slowly in time) if there is a time-of-flight (*d*-spacing) independent term in the background function. However, the delayed neutrons can lead to significant errors in the incident spectrum. An incident spectrum containing only the prompt neutrons is needed to normalize Bragg intensities. Thus, the delayed neutrons must be accurately subtracted from the measured incident spectrum before it can be used for analysis.

The method we have described for measuring the incident spectrum results in a measurement that contains only slow delayed neutrons (i.e., those with energies below the cadmium cutoff energy). Fast delayed neutrons pass through both the cadmium with the pin-hole and the solid sheet of cadmium, and are thus subtracted out with the other contributions to background. The fast delayed neutrons appear as a constant neutron flux in the background spectrum (counted through the cadmium sheet) for long times-of-flight where the cadmium absorbs prompt neutrons (see Fig. 2).

We have used two methods for determining the contribution of slow delayed neutrons. The first assumes that the moderation is essentially complete at long wavelengths. Thus, we fit the "tail" of the spectrum (*e.g.* above 25000 μs) with the asymptotic form of a Maxwellian plus a constant term for the delayed neutrons:

$$I_t = n_{sd} + A/t^5 \qquad (4)$$

where n_{sd} is the background count of slow delayed neutrons and A/t^5 describes the time-dependent neutron flux as a function of time-of-flight, t. The slow delayed neutrons are then subtracted to obtained an incident spectrum suitable for use in Rietveld refinement. If this correction for slow delayed neutrons were not applied, the final spectrum would possess an error of approximately 1% at 15000 μs rising to greater than 15% at 30000 μs.

When the transmitted beam incident spectrum has been collected with a special environment apparatus, *e.g.* a pressure or furnace, in place, attenuation of the neutron beam occurs and must be included in the fitting procedure, yielding the equation:

$$I_t = n_{sd} + Ae^{-Bt}/t^5 \qquad (5)$$

here the e^{-Bt} term accounts for absorption.

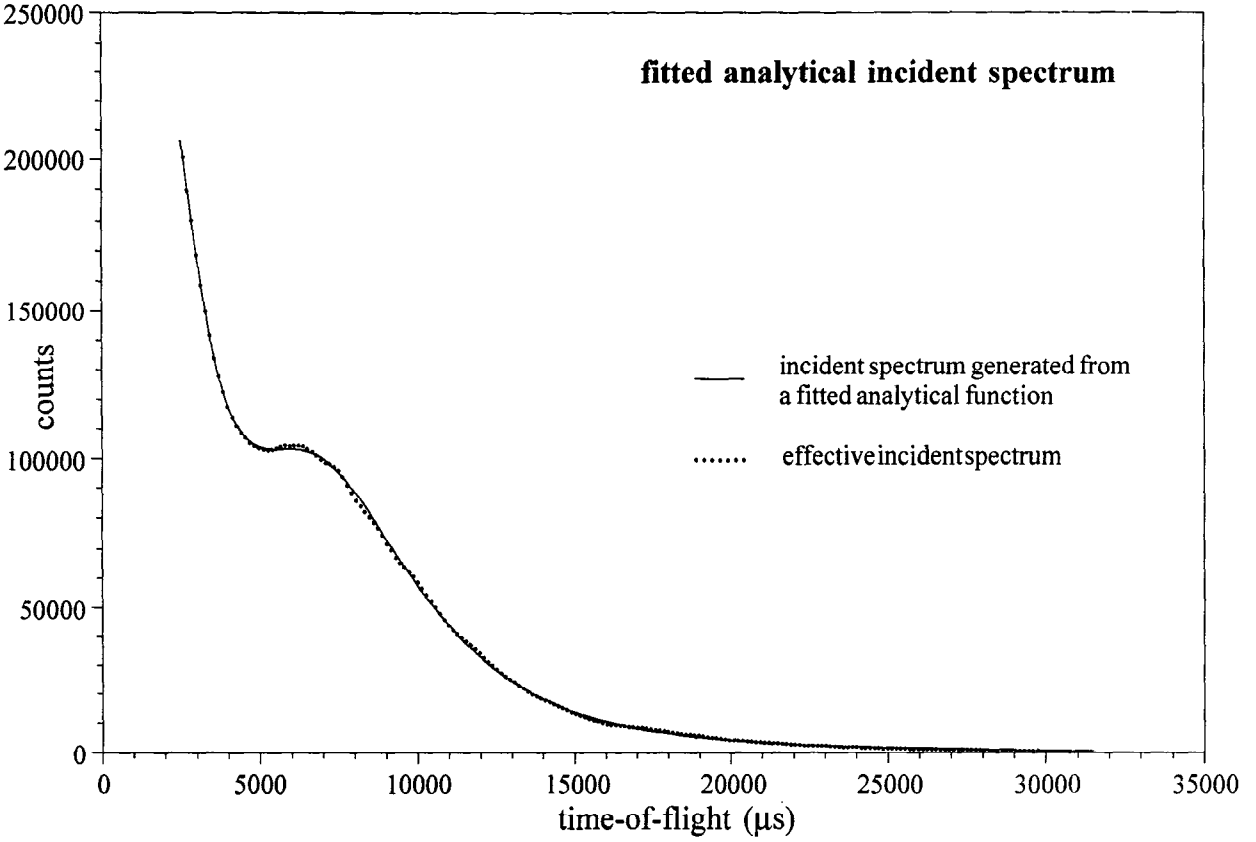

Fig. 5. An analytical incident spectrum that has not accounted for Bragg cutoffs and slow delayed neutrons plotted against the previously constructed effective incident spectrum.

conditions for the upper limit (j_{max}) of the summing operation, eq. 3, can not be met at long times. Fortunately, the shape of the incident spectrum at long times is well defined by eq. 4 or 5 and this can be used to extrapolate the effective incident spectrum to times that correspond to the data frame, as shown in Fig. 4.

5. Results

In order to illustrate the magnitude of error that arises from not accounting for Bragg cutoffs and delayed neutrons in the incident spectrum, it is interesting to compare the effective incident spectrum with an incident spectrum defined by a smooth analytical function as is often used in Rietveld refinement codes [3,4]:

$$I_t = P_1 + P_2 e^{-(P_3/t^2)/t^5} + P_4 e^{-(P_5 t^2)} + P_6 e^{-(P_7 t^3)} + P_8 e^{-(P_9 t^4)} \qquad (6)$$

In Fig. 5, an analytical incident spectrum derived from fitting the time-focused incident spectrum before correction for delayed neutrons is plotted against the effective incident spectrum. Clearly, the analytical incident spectrum has the general shape of the effective spectrum, and it may

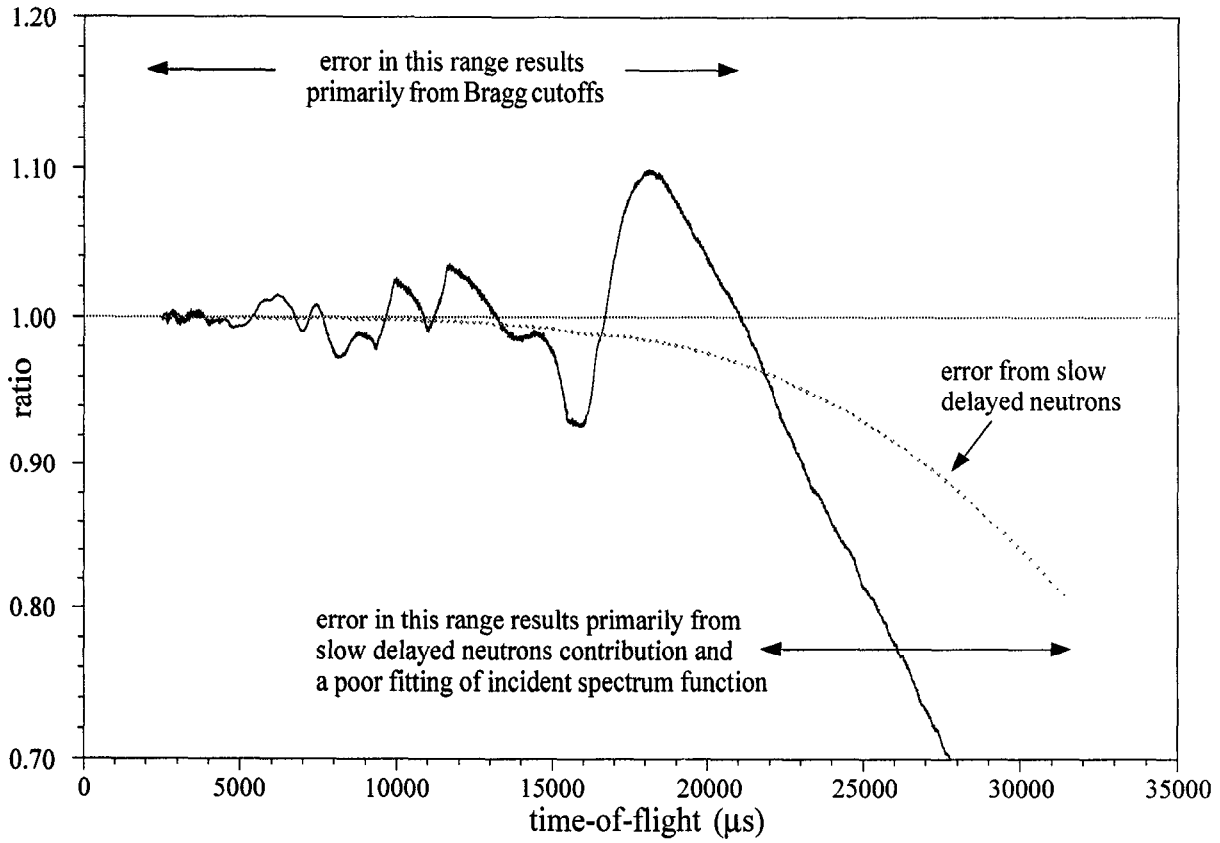

Fig. 6. The ratio of the effective incident spectrum to the analytical incident spectrum function, which illustrates the significant differences between them.

therefore appear that the differences between the two spectra are of minor significance. However, when one considers the ratio of these two spectra, as plotted in Fig. 6, the error that would be introduced in the estimates of relative peak intensities in a Rietveld refinement is evident. This error, deviance from unity in Fig. 6, results from excluding the effects of Bragg cutoffs and slow delayed neutrons, and is then compounded by a poor fitting of the analytical function to the tail of the incident spectrum. Clearly, the magnitude of error is very significant with regard to intended precise analysis of diffraction data.

6. Conclusion

To conclude, it is evident that in order to construct an effective incident spectrum, one must include the effects of Bragg cutoffs from window material, and the time independent background of delayed neutrons. The method outlined above achieves these aims by adopting a numerical, rather than analytical, approach for the construction of an effective incident spectrum. A particular advantage of this method, is its ability to easily accommodate different sample environments, *i.e.* the use of a pressure cell, a furnace *etc.*.

Acknowledgment

Work at Argonne National Laboratory is supported by the U.S. D.O.E., Basic Energy Sciences - Materials Sciences, under contract W-31-109-Eng-38.

References

1. J. D. Jorgensen and F. J. Rotella, High-Resolution Time-of-Flight Powder Diffractometer at the ZING-P' Pulsed Neutron Source, *J. Appl. Crystallogr.* 15, 27 (1982).
2. J. D. Jorgensen, J. Faber, Jr., J. M. Carpenter, R. K. Crawford, J. R. Haumann, R. L. Hitterman, R. Kleb, G. E. Ostrowski, F. J. Rotella, T. G. Worlton, Electronically Focused Time-of-Flight Powder Diffractometers at the Intense Pulsed Neutron Source, *J. Appl. Crystallogr.* 22, 321 (1989).
3. R. B. Von Dreele, J. D. Jorgensen, C. G. Windsor, Rietveld Refinement with Spallation Neutron Powder Diffraction Data, *J. Appl. Crystallogr.* 15, 581 (1982).
4. It should be noted that several alternative functions are available in recent Rietveld codes, such as GSAS, but none of them can fit the sharp features resulting from Bragg cutoffs.